

Glycogen synthase kinase-3 β ablation limits pancreatitis-induced acinar-to-ductal metaplasia

Li Ding¹, Geou-Yarh Liou^{2,†}, Daniel M Schmitt³, Peter Storz², Jin-San Zhang^{1,4,*} and Daniel D Billadeau^{1,*} 

¹ Division of Oncology Research and Schulze Center for Novel Therapeutics, Mayo Clinic, Rochester, MN, USA

² Department of Cancer Biology, Mayo Clinic, Jacksonville, FL, USA

³ Actuate Therapeutics, Fort Worth, TX, USA

⁴ Key Laboratory of Biotechnology and Pharmaceutical Engineering, School of Pharmaceutical Sciences, and Center for Precision Medicine, The First Affiliated Hospital, Wenzhou Medical University; Institute of Life Sciences, Wenzhou University, Wenzhou, Zhejiang, China

*Correspondence to: Jin-San Zhang or Daniel D Billadeau, Division of Oncology Research and Schulze Center for Novel Therapeutics, Mayo Clinic, 200 First St SW, Rochester, MN, USA. E-mail: zhangjinsan@mayo.edu or billadeau.daniel@mayo.edu.

†Current address: Center for Cancer Research and Therapeutic Development, Department of Biological Sciences, Clark Atlanta University, Atlanta, GA 30314, USA.

Abstract

Acinar-to-ductal metaplasia (ADM) is a reversible epithelial transdifferentiation process that occurs in the pancreas in response to acute inflammation. ADM can rapidly progress towards pre-malignant pancreatic intraepithelial neoplasia (PanIN) lesions in the presence of mutant KRas and ultimately pancreatic adenocarcinoma (PDAC). In the present work, we elucidate the role and related mechanism of glycogen synthase kinase-3 β (GSK-3 β) in ADM development using *in vitro* 3D cultures and genetically engineered mouse models. We show that GSK-3 β promotes TGF- α -induced ADM in 3D cultured primary acinar cells, whereas deletion of GSK-3 β attenuates caerulein-induced ADM formation and PanIN progression in *Kras*^{G12D} transgenic mice. Furthermore, we demonstrate that GSK-3 β ablation influences ADM formation and PanIN progression by suppressing oncogenic KRas-driven cell proliferation. Mechanistically, we show that GSK-3 β regulates proliferation by increasing the activation of S6 kinase. Taken together, these results indicate that GSK-3 β participates in early pancreatitis-induced ADM and thus could be a target for the treatment of chronic pancreatitis and the prevention of PDAC progression.

Copyright © 2017 Pathological Society of Great Britain and Ireland. Published by John Wiley & Sons, Ltd.

Keywords: pancreatic cancer; pancreatitis; acinar-to-ductal metaplasia; glycogen synthase kinase-3 β ; KRas; S6 K

Received 4 February 2017; Revised 1 June 2017; Accepted 13 June 2017

Conflict of interest statement: DMS is CEO of Actuate Therapeutics Inc and has ownership interest in Actuate Therapeutics Inc. DDB has ownership interest in Actuate Therapeutics Inc. The other authors disclosed no potential conflicts of interest.

Introduction

Pancreatic ductal adenocarcinoma (PDAC) is among the most deadly human malignancies [1–3]. Oncogenic KRAS mutation represents the most frequent and earliest genetic alteration in PDAC patients, highlighting its role as a driver of PDAC [4,5]. Indeed, genetically engineered mouse models expressing activated mutant KRas (G12D) in the pancreas develop pancreatic cancer with a long latency, which can be substantially accelerated by experimentally inducing chronic pancreatitis through the administration of the CCK agonist caerulein [6–8]. Several studies have shown that inflammation and aberrant growth factor signalling can drive acinar cells to dedifferentiate into metaplastic duct-like cells, a process termed acinar-to-ductal metaplasia (ADM) [8–10]. Interestingly, lineage-tracing experiments in these models have demonstrated that preneoplastic pancreatic intraepithelial neoplasia (PanIN) lesions are mainly

derived from acinar cells undergoing ADM [4,11–13]. Although ADM is a benign lesion and a reversible process [14,15], the presence of mutant KRas ‘locks’ the metaplastic cells in a duct-like state, suggesting that ADM might be an early event that interacts with mutant KRas to promote PDAC development.

Glycogen synthase kinase-3 (GSK3) α and β are highly conserved serine–threonine kinases involved in several cellular functions including glycogen metabolism, Wnt/ β -catenin signalling, immune regulation, and maintenance of stem cell identity [16,17]. Not surprisingly, these two kinases participate in the pathogenesis of various human diseases, such as diabetes and inflammatory and neurological disorders, as well as cancer [18,19]. Reports from our and other groups have indicated that GSK-3 β is progressively overexpressed from PanIN to advanced PDAC, and becomes nuclear accumulated in most moderately and poorly differentiated tumours [20,21]. Significantly,

GSK-3 β overexpression contributes to PDAC cell proliferation and survival, whereas GSK-3 inhibition reduces pancreatic cancer cell viability *in vitro* and suppresses tumour xenograft growth *in vivo* [22,23]. Lastly, oncogenic *KRas* signalling regulates GSK-3 β gene expression, suggesting that GSK-3 β may be important for *KRas*-driven tumour-promoting pathways during the development of PDAC [24].

Although most studies have shown functional redundancy between the two homologues of GSK-3, as exemplified by their regulation of Wnt/ β -catenin signalling, they also exhibit tissue-specific functions that may have varying impact on human cancer aetiology [25,26]. We have previously demonstrated that the two GSK-3 isoforms exhibit differential activity towards TRAIL (tumour necrosis factor α -related apoptosis-inducing ligand)- or TNF α -induced apoptosis in PDAC cells [27]. Significantly, addition of a GSK-3 inhibitor concomitantly with caerulein prevented the onset of ADM in a dose-dependent manner [28]. However, the role of GSK-3 β in early PDAC, especially pancreatitis-induced ADM, remains unknown.

Herein, we provide evidence that GSK-3 β is necessary for oncogenic *KRas*-mediated formation of duct-like structures *in vitro*. Moreover, conditional deletion of *Gsk3b* in *Pdx1-Cre;LSL-Kras^{G12D}* mice abrogated caerulein-induced ADM, PanIN lesion formation, inflammation, and fibrosis. Significantly, *Gsk3b* deletion resulted in a substantial decrease in the number of proliferating cells within ADM and PanIN areas. Mechanistically, we find enhanced activation of S6 kinase (S6K) resulting in the elevated phosphorylation of S6 in ADM and PanIN epithelial cells, which is substantially reduced in the absence of GSK-3 β . As ADM is an early event contributing to the development of PDAC, our data suggest that pharmacological inhibition of GSK-3 may be an effective strategy to prevent early changes that are required for further development to PDAC.

Materials and methods

Reagents, cell culture, and drug treatment

Caerulein, DMSO, and other chemicals were obtained from Sigma (St Louis, MO, USA) unless otherwise specified. The GSK-3 inhibitor 9-ING-41 (GSK-3i) was obtained from Actuate Therapeutics (Fort Worth, TX, USA). Recombinant human TGF- α was obtained from R&D Systems (Minneapolis, MN, USA). Soybean trypsin inhibitor was obtained from Affymetrix (Santa Clara, CA, USA). Rat-tail collagen I was obtained from BD (Franklin Lakes, NJ, USA). AR42J cells were passaged in Ham's F-12 K (Kaighn's) medium supplemented with 15% fetal bovine serum (FBS), 2 mM L-glutamine, and penicillin/streptomycin. For caerulein stimulation experiments, cells were serum-starved for 16 h and pretreated with 9ING41 (500 nM) for 2 h, then

10 nM caerulein for 2 or 6 h. Stable shGSK-3 β or scramble AR42J cells were fasted overnight prior to caerulein (10 nM) stimulation. Cells were harvested 2, 6, and 12 h post-caerulein stimulation.

Lentiviral packaging, transduction, and selection of stable cells

Lentivirus packaging, cell infection, and selection of pLKO-shRNA stable cells were performed as previously described following institutional biosafety regulations [27]. AR42J cells were infected with appropriate amounts of lentiviral particles containing medium. Twenty-four hours later, virus-containing medium was removed and replaced with fresh medium supplemented with 2 μ g/ml puromycin. Pooled resistant clones were used for experiments.

Animals and acute pancreatitis model

Experimental animals were generated by crossing *Pdx1-Cre;LSL-Kras^{G12D}* mice with *Gsk3b^{F/F}* mice. To induce pancreatitis, 6-week-old male sibling littermates from each genotype were selected for treatment. Mice were starved for 12 h and allowed water *ad libitum* 1 day prior to the experiment. Animals were injected intraperitoneally into the right lower quadrant with 50 μ g/kg body weight caerulein dissolved in 0.9% saline in a volume of 100 μ l. Injections were given at hourly intervals up to eight times. Pancreata were harvested 2 and 7 days after caerulein treatment. All animal experiments were approved by the Mayo Clinic Institutional Animal Care and Use Committee and were performed in accordance with relevant institutional and national guidelines and regulations.

3D explant culture *in vitro*

Primary pancreatic acinar cells were isolated as previously described [29,30]. Briefly, the pancreas was washed in cold serum-free Hank's Balanced Salt Solution, cut into 1–2 mm pieces, and digested with collagenase I. Small clusters of acinar cells were filtered through a 100 μ m cell strainer and further purified with density gradient centrifugation, and resuspended in complete Waymouth medium (10% FBS, 0.1 mg/ml trypsin inhibitor, and 1 μ g/ml dexamethasone). Freshly isolated acinar cells were then mixed with an equal volume of collagen solution and seeded in cell culture plates precoated with collagen I in Waymouth medium. Following 15–30 min incubation at 37 $^{\circ}$ C, another layer of Waymouth complete medium with or without TGF- α or GSK-3 inhibitors was added. To express proteins using the lentiviral expression system, acinar cells were infected with an appropriate amount of packaged viral particles and incubated for 3–5 h before embedding in the collagen I/medium mixture. At day 6 or 7 (dependent on the time course of duct formation), the number of ducts was counted under a microscope.

Immunohistochemistry, EdU labelling, and immunofluorescence

Following caerulein treatment, mice were anaesthetized using isoflurane (Piramal Critical Care Inc, Bethlehem, PA, USA), followed by cervical dislocation. The whole pancreas was quickly removed and fixed overnight in 4% PFA with gentle shaking, embedded in paraffin, and cut into 5- μ m-thick sections. Sections were subjected to haematoxylin and eosin (H&E) staining, immunohistochemistry (IHC), and immunofluorescence staining as previously described [31] (see supplementary material, Table S1, for antibody sources and dilutions). For EdU labelling, mice were injected with EdU at a concentration of 50 mg/kg per body weight in saline 2 h before sacrifice. Staining was performed by a Click-iT[®] EdU Alexa Fluor[®] 488 Imaging Kit following the manufacturer's instructions (Thermo Fisher Scientific, Waltham, MA, USA). Confocal images were collected with an LSM-710 laser scanning confocal microscope with a 63 \times water Plan-Apochromat objective lens using ZEN 2009 software (Carl Zeiss, Oberkochen, Germany).

Western blot analysis, quantitative RT-PCR, and Qiagen RT² PCR array

Snap-frozen pancreata from mice of desired genotypes were homogenized in RIPA buffer (Abcam, Cambridge, MA, USA). Protein extracts were prepared, separated by SDS-PAGE, transferred to PVDF membrane, and immunoblotted as previously described [24]. Antibody details are provided in the supplementary material, Table S1. Protein bands of interest were quantified by calculating an integrated density value for each band using ImageJ (National Institutes of Health, Bethesda, MD, USA). Pancreatic total RNA was isolated using Trizol and further purified with an RNeasy Mini Kit (Qiagen, Valencia, CA, USA). Reverse transcription was performed with the Superscript III RT-PCR Kit (Invitrogen, Carlsbad, CA, USA). Quantitative PCR was performed with the SYBR Green PCR Master Mix using the ABI StepOnePlus Sequence Detection System (Applied Biosystems, Carlsbad, CA, USA). *Gapdh* and *Rplp0* were used as housekeeping genes for normalization of gene expression. *Ccnd1* and *Myc* were analysed using the Qiagen RT² PCR array kit (PAMM-225Z; Qiagen) that contains five internal controls for gene expression. The double delta Ct method was used to analyse gene expression. Experiments were performed in triplicate using three independent cDNAs. Primer sequences are provided in the supplementary material, Table S2.

Statistical analysis

Data are presented as mean \pm SEM and were analysed by repeated measures analysis of variance and unpaired Student's *t*-test using GraphPad Prism software (GraphPad Software Inc, La Jolla, CA, USA). A value of $p < 0.05$ denotes statistical significance.

Results

GSK-3 β expression is increased following caerulein-induced pancreatitis in mice

Pancreatic tissues sections from control- or caerulein-treated *Pdx1-Cre* and *Pdx1-Cre;LSL-Kras^{G12D}* mice were stained for GSK-3 β expression following caerulein-induced pancreatitis. GSK-3 β was weakly cytoplasmic in saline-treated *Pdx1-Cre* mice, but was increased in areas of ADM by 2 days post-caerulein treatment (Figure 1A). Similar to our previous data, GSK-3 β was elevated in *Pdx1-Cre;LSL-Kras^{G12D}* mice and was increased further upon caerulein treatment (Figure 1A). In addition, protein extracts demonstrated increased levels GSK-3 β compared with control mice and slightly increased levels of GSK-3 β following the administration of caerulein (Figure 1B, C). We also noted increased levels of GSK-3 α in control and *Pdx1-Cre;LSL-Kras^{G12D}* mice following caerulein treatment, suggesting that this kinase may also be linked to oncogenic *KRas^{G12D}* signalling (Figure 1B, C). Overall, these data indicate that the expression levels of both GSK-3 kinase isoforms are increased in response to caerulein-induced pancreatitis and oncogenic *KRas^{G12D}* signalling.

GSK-3 β promotes TGF- α -induced ADM

To investigate whether GSK-3 kinases are involved in ADM, we cultured isolated mouse pancreatic acinar cells in collagen. This *ex vivo* explant model for ADM is based on a previously established cell culture model in which growth factors such as TGF- α that activate the EGF receptor ErbB1 have been shown to induce ADM within 6–8 days [30]. Consistent with this, TGF- α stimulation of primary acinar cells resulted in a three-fold increase in ADM events (Figure 2A, B and supplementary material, Figure S1). Addition of a GSK-3 inhibitor (GSK-3i) slightly reduced the number of ADM events in unstimulated cells, but substantially impaired TGF- α -induced ductal formation, showing a six-fold decrease (Figure 2A, B and supplementary material, Figure S1). Taken together, these data indicate that GSK-3 kinases are involved in the process of ADM *in vitro*.

Since the GSK-3i can inhibit both GSK-3 kinases, we next sought to determine whether GSK-3 β was necessary for TGF- α -induced ADM. First, using an shRNA lentivirus targeting *Gsk3b*, we infected isolated acinar cells and then left them unstimulated or stimulated them with TGF- α for 6 days. Knockdown of GSK-3 β resulted in a 12-fold decrease in ductal formation compared with scrambled control (Figure 2C). Furthermore, ectopic expression of a constitutively active GSK-3 β (S9A) promoted ductal formation even in the absence of TGF- α (Figure 2D). Lastly, we isolated acinar cells from *Pdx1-Cre* and *Pdx1-Cre;Gsk3b^{F/F}* mice and examined TGF- α -induced ADM *ex vivo*. As shown in Figure 2E, F, acinar cells from *Gsk3b* knockout animals

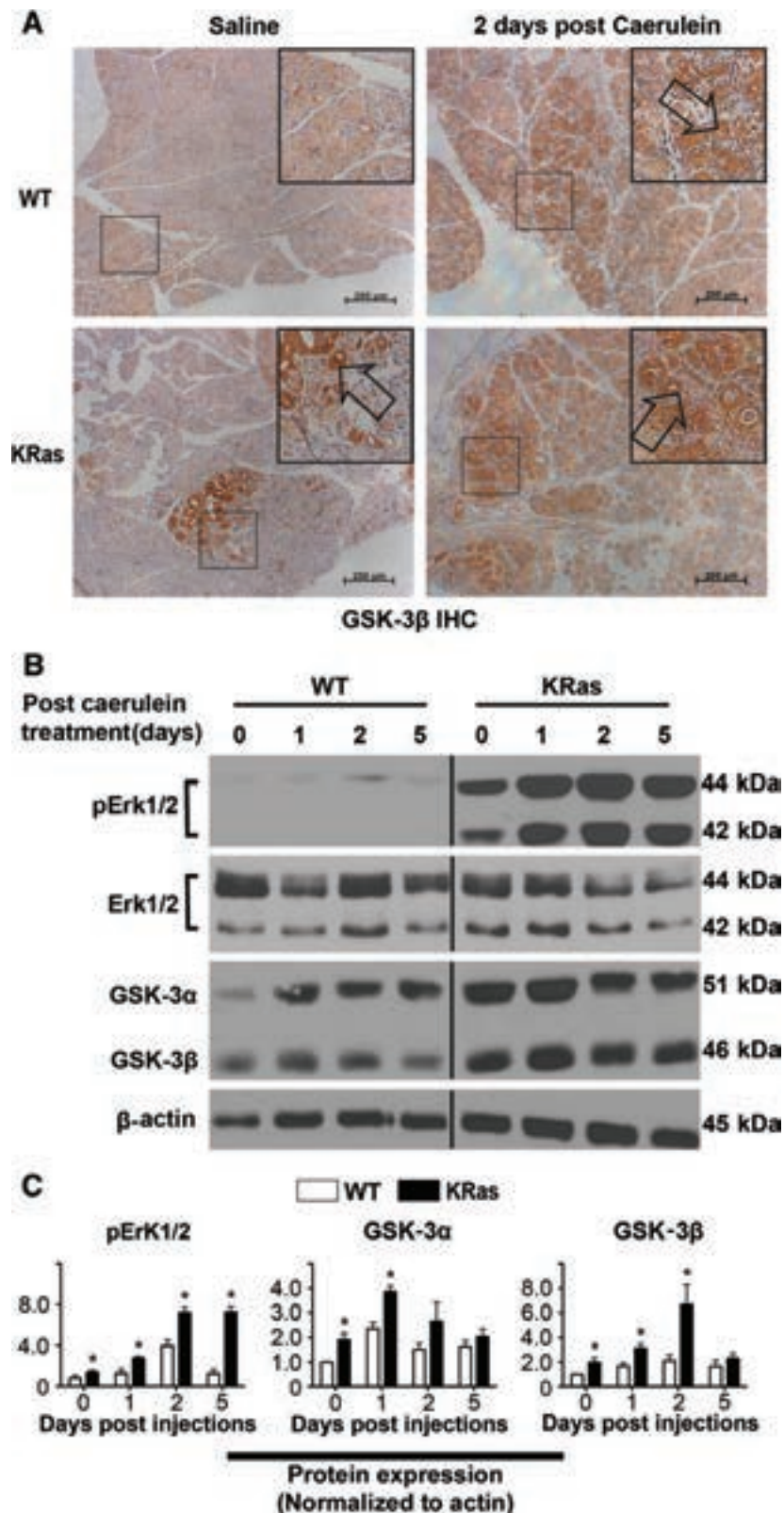


Figure 1. GSK-3 β protein expression is elevated following caerulein-induced pancreatitis in mice. (A) Representative IHC images of GSK-3 β in pancreatic sections from *Pdx1-Cre* wild-type (WT) (upper panel) and *Pdx1-Cre;LSL-KRas^{G12D}* (KRas) mice (lower panel) treated with or without caerulein. Arrows point to the abnormal pancreas area. Bars = 200 μ m. (B) Immunoblots for phosphorylated Erk1/2, total Erk1/2, GSK-3 α , and GSK-3 β in pancreatic tissue of WT and KRas mice before and 1, 2, and 5 days post-caerulein treatment. β -Actin was used as a loading control. The black vertical line in B denotes where an additional time point was removed. Samples were developed from the same membrane. Representative results are shown from three experiments. (C) The average signal intensity of phospho-Erk1/2, GSK-3 α , and GSK-3 β was quantified and is expressed as mean \pm SEM ($n = 3$). * $p < 0.05$ KRas versus WT mice.

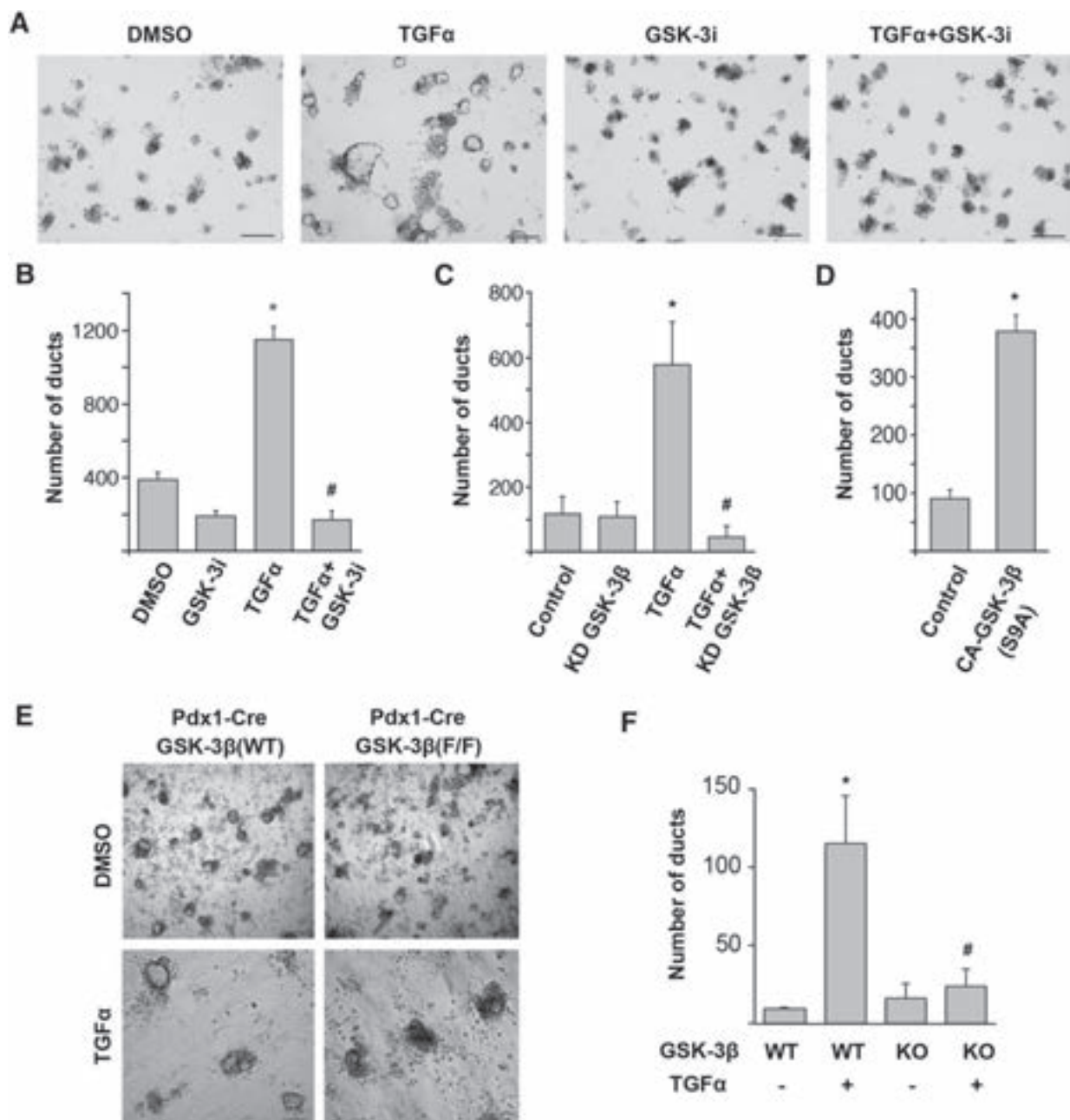


Figure 2. GSK-3 β promotes TGF- α -induced ADM. (A) Freshly isolated primary mouse acinar cells were embedded in a 3D collagen culture. Images show acinar cell clusters or ducts on day 6 following treatment with DMSO, 50 ng/ml TGF- α , 1 μ M GSK-3i or 50 ng/ml TGF- α combined with 1 μ M GSK-3i. Bars = 250 μ m. (B) Effect of GSK-3 inhibition on TGF- α -induced ADM *in vitro*. The number of ducts was quantified by counting. * p < 0.05 TGF- α versus DMSO; # p < 0.05 TGF- α combined with GSK-3i versus TGF- α only. (C) Primary mouse pancreatic acinar cells were isolated, transduced with GSK-3 β kinase-dead (KD) lentiviral particles, and seeded in collagen with or without TGF- α (50 ng/ml). The number of ducts formed was enumerated on day 6 post-stimulation. * p < 0.05 TGF- α versus control; # p < 0.05 TGF- α combined with kinase-dead (KD) mutant versus TGF- α only. (D) Primary mouse pancreatic acinar cells were isolated, transduced with constitutively active GSK-3 β (S9A) lentiviral particles, and seeded in collagen. The number of ducts formed was enumerated on day 6 post-stimulation. * p < 0.05 TGF- α or constitutively active GSK-3 β (S9A) versus control; # p < 0.05 TGF- α combined with kinase-dead (KD) mutant versus TGF- α only. (E) Primary acinar cells from *Pdx1-Cre;GSK-3 β (WT)* and *Pdx1-Cre;GSK-3 β ^{F/F}* (KO) mice were isolated and cultured for 6 days in collagen in the presence of DMSO or TGF- α , 50 ng/ml. Representative images of ductal-like structures are shown. Bars = 250 μ m. (F) Quantification of ducts formed following 6 days of stimulation. * p < 0.05 TGF- α treated versus untreated WT acinar cells; # p < 0.05 TGF- α treated KO acinar cells versus WT acinar cells. All experiments were repeated using acinar cells derived from at least three different mice. Data were analysed and are expressed as mean \pm SEM. n = 15.

had significantly diminished duct-forming ability under TGF- α stimulation compared with WT acinar cells. Overall, these data suggest that GSK-3 β is an important signalling molecule involved in TGF- α -induced ADM *in vitro*.

Generation of *Pdx1-Cre;LSL-Kras^{G12D};Gsk3b^{F/F}* compound mouse strain

To further define the role of GSK-3 β in the process of ADM in the context of the oncogenic *KRas*, we generated pancreas-specific *Gsk3b* knockout mice harbouring

oncogenic *Kras* (*Pdx1-Cre;LSL-Kras*^{G12D};*Gsk3b*^{F/F}). To confirm the successful deletion of *Gsk3b*, we isolated protein from the pancreas of pairs of *Pdx1-Cre* (WT), *Pdx1-Cre;LSL-Kras*^{G12D} (KRas), *Pdx1-Cre;Gsk3b*^{F/F} (KO), and *Pdx1-Cre;LSL-Kras*^{G12D};*Gsk3b*^{F/F} (RKO) mice. Protein extracts from both KO and RKO animals showed a loss of both phosphorylated and total GSK-3 β compared with WT and KRas mice (Figure 3A, B). Consistent with a prior study [32], we did not observe an up-regulation of GSK-3 α or β -catenin protein levels upon loss of GSK-3 β (Figure 3A). Furthermore, KO and RKO animals showed neither nuclear translocation of β -catenin nor induced expression of two well-known target genes (*Myc* or *Ccnd1*) compared with WT and KRas animals (supplementary material, Figure S2A, B). IHC confirmed that GSK-3 β was widely expressed in both endocrine and exocrine cells within the pancreas. Similar to the immunoblot results, GSK-3 β staining was reduced in the KO and RKO animals (Figure 3C). Consistent with the data shown in Figure 1A, we found aberrant accumulation of GSK-3 β in pancreatic cancer precursor lesions in KRas mice (Figure 3C, KRas panel). Thus, we used this model to evaluate the contribution of GSK-3 β to the process of ADM *in vivo*.

GSK-3 β is necessary for KRas-mediated ADM *in vivo*
Caerulein has been used to induce acute pancreatitis in various animal models harbouring oncogenic *Kras*^{G12D} [33]. Interestingly, in addition to preventing conversion of metaplastic ductal cells back to acinar cells following the resolution of pancreatitis, mice harbouring oncogenic *Kras* develop more advanced PanIN lesions and ultimately PDAC [6,33]. To test the impact of GSK-3 β deletion alone or in the context of oncogenic *KRas* on acinar cell recovery and PanIN progression, we injected saline or caerulein as indicated in Figure 4A and harvested pancreata on days 2 and 7. Saline-injected mice showed no gross pathological changes in any genotype (Figure 4B, top panel). However, compared with WT mice, gross pathological examination revealed hallmarks of severe pancreatitis in caerulein-treated KRas mice, including a gelatinous change of the pancreas, oedema and swelling by day 2, and the formation of a dense desmoplastic reaction by day 7 (Figure 4B). In contrast, there were no significant differences between KO and WT mice that had been treated with caerulein. Interestingly, the grade of pancreatitis was macroscopically reduced in RKO mice, with less oedema, swelling, and desmoplasia at 2 and 7 days post-caerulein injection compared with KRas mice (Figure 4B). Histologically, WT and KO mice had limited areas of pancreatitis at day 2 post-caerulein injection (Figure 4C and supplementary material, Figure S3A), which mostly resolved by day 7. In contrast, KRas mice showed extensive areas of pancreatitis at day 2 and further development of ADM and PanIN regions by day 7 along with extensive desmoplasia (Figure 4C, KRas panel). Alcian blue staining further confirmed the reduction of ADM formation and

PanIN progression in RKO mice (supplementary material, Figure S3B).

Amylase and CK19 are commonly used markers of acinar and ductal cells in the pancreas, respectively. The co-existence of their staining within the same area indicates the loss of acinar identity and transdifferentiation into ductal cells [11]. As determined by immunofluorescence and the expression of the ductal markers CK7 and CK19, WT and KO mice have very little to no areas of spontaneous ADM, which increases modestly in response to caerulein treatment and is mostly resolved by day 7 (Figure 4C–E and supplementary material, Figure S3A). Consistent with previous reports, KRas mice showed higher levels of spontaneous ADM in saline-treated animals, as well as a dramatic increase in ADM and desmoplasia by day 2, which continued into day 7 (Figure 4C, D). The decrease in ADM area by day 7 in KRas mice is accounted for by the increase in PanIN lesion formation (supplementary material, Figure S3C). The expression of CK7 and CK19 levels also remained elevated at day 7, consistent with the increase in ADM and PanIN areas in KRas mice (Figure 4E). In contrast, the pancreas in saline-treated RKO mice was composed of mostly acinar cells and, importantly, fewer spontaneous ADM areas (3.0 ± 0.3 versus $6.2 \pm 0.2\%$ of ADM area/total pancreas; Figure 4C). Upon caerulein exposure, ADM areas with abnormal ductal structures were reduced in RKO mice compared with KRas mice (7.7 ± 1.6 versus $18.8 \pm 5.2\%$ of ADM area/total pancreas) (Figure 4C, D and supplementary material, Figure S3D). Seven days post-treatment, ADM progression was limited in RKO mice compared with KRas mice (3.2 ± 2.2 versus 11.2 ± 2.5) and more amylase-positive acinar cells remained compared with CK19- and CK7-expressing ductal cells (Figure 4C–E). Taken together, these data reveal an important role for GSK-3 β in the maintenance/progression of ADM to PanIN formation.

GSK-3 β contributes to cell proliferation within ADM and PanIN lesions

Normally, alpha-smooth muscle actin (α SMA) is associated with blood vessels but not ductal structures in WT mice (supplementary material, Figure S4A). However, α SMA becomes associated with metaplastic ducts and PanIN lesions (supplementary material, Figure S4A) [34]. Previous studies have shown that acinar and ductal cells are proliferatively quiescent in the WT pancreas [11,35]. During ADM, *KRas* mutation activates a proliferation programme resulting in a subset of cells progressing towards a duct cell phenotype. Significantly, we could observe α SMA⁺/Ki-67⁺/CK19⁺ ductal cells within areas of ADM from KRas mice, but not in CK19⁺/ α SMA⁻ normal ductal cells (supplementary material, Figure S4B). As shown in Figure 5A, several Ki-67-positive cells were detected in ADM areas in KRas mice 2 days after caerulein injection with a dramatic accumulation of Ki-67 positive cells in PanIN lesions 7 days after caerulein injection. In

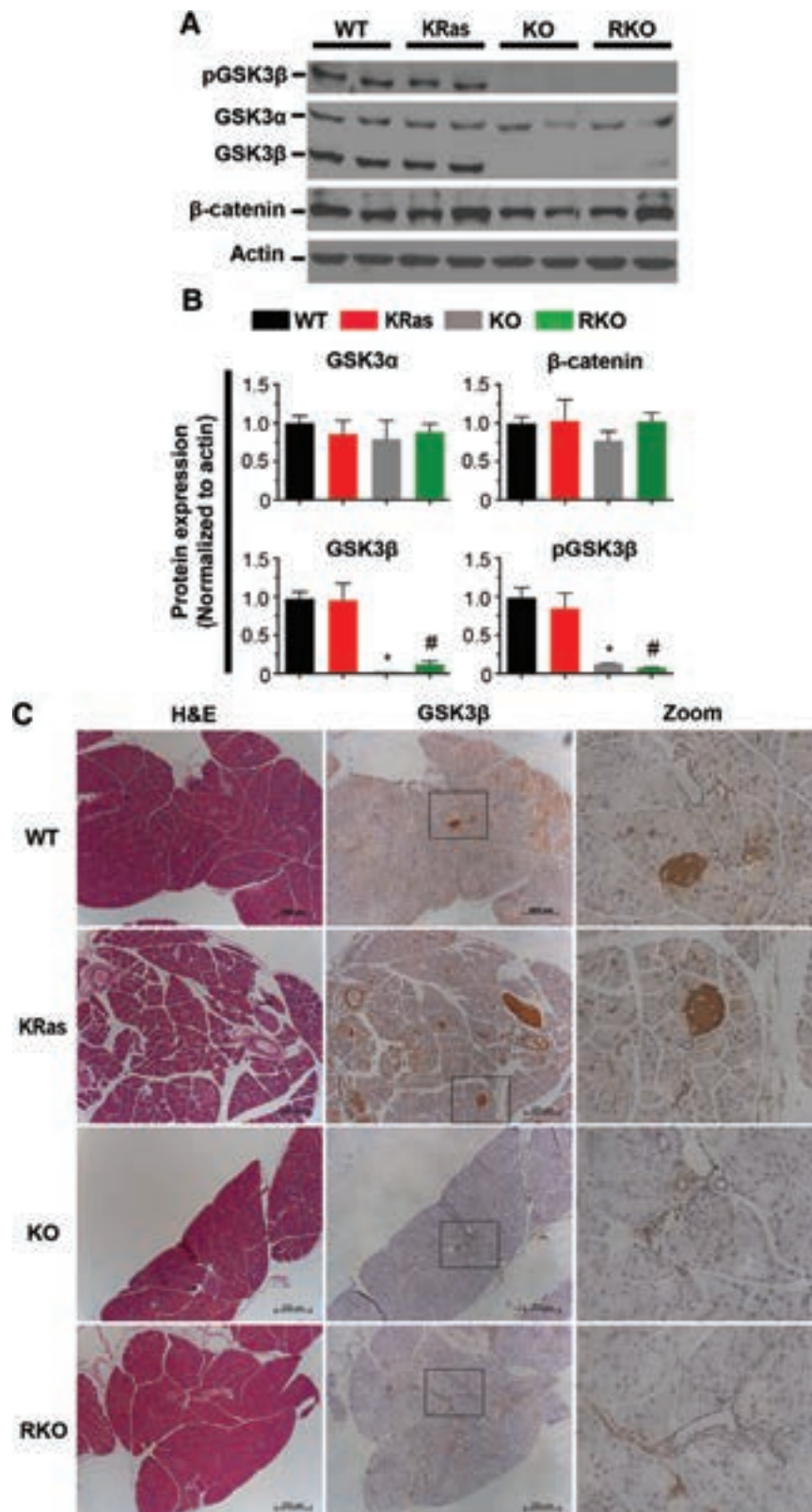


Figure 3. Deletion of GSK-3 β in the pancreas of genetically engineered mice. (A) *Pdx1-Cre*, *LSL-KRas^{G12D}*, and *GSK-3 β ^{Fl/Fl}* mice were used to generate mice of desired genotypes as described in the Materials and methods section. The levels of phospho-GSK-3 β (Ser9), GSK-3 α/β , and β -catenin in pancreatic tissues were examined by immunoblot. β -Actin was used as a loading control. Representative results from six experiments are shown. (B) Signal intensities of phospho-GSK-3 β (Ser9), GSK-3 α/β , and β -catenin (mean \pm SEM, $n = 6$). * $p < 0.05$ KO versus WT mice; # $p < 0.05$ RKO versus KRas mice. (C) H&E staining and IHC of GSK-3 β in pancreas sections of WT, KRas, KO, and RKO mice. Representative images were taken under low and high magnification lens. Bars = 200 μ m.

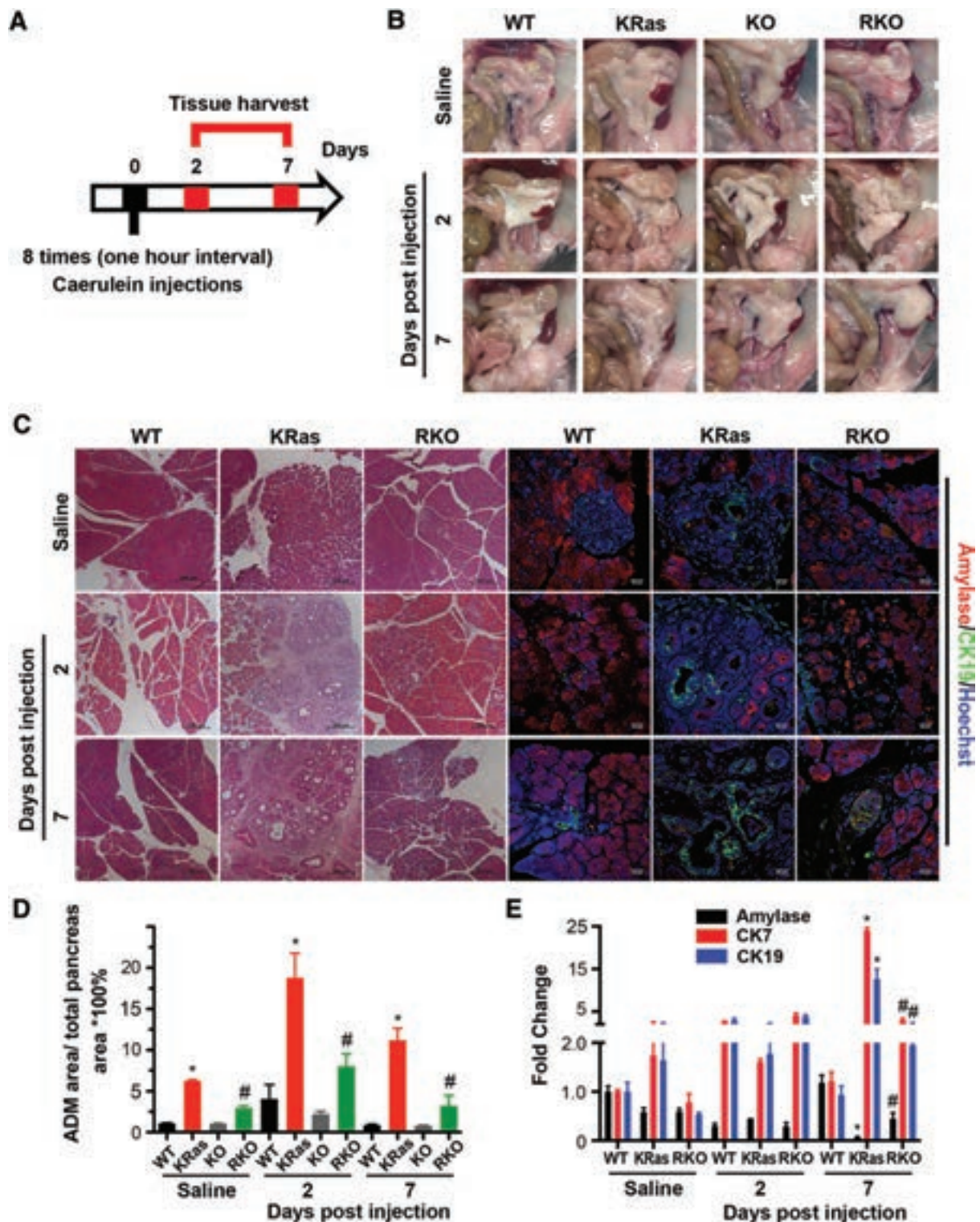


Figure 4. GSK-3 β is necessary for KRas-initiated ADM *in vivo*. (A) Scheme for caerulein-induced acute pancreatitis model and analysis. (B) Gross pathology of pancreas and adjacent tissues from transgenic mice of indicated genotypes treated with saline or 2 and 7 days post-caerulein injection. (C) H&E-stained pancreatic sections from WT, KRas, and RKO mice (left panel) and immunofluorescence staining of amylase and CK19 (right panel) of mice treated with saline or 2 and 7 days post-caerulein injection. Nuclei were counterstained with Hoechst (blue). (D) H&E-stained tissue samples from WT (black), KRas (red), KO (grey), and RKO (green) mice were quantitatively analysed for the ADM area as a percentage to the total area (mean \pm SEM, $n = 25$). * $p < 0.05$ KRas versus WT mice; # $p < 0.05$ RKO versus KRas mice. (E) Real-time PCR quantification of pancreatic gene expression for amylase (black), CK7 (red), and CK19 (blue) from WT, KRas or RKO mice treated with saline or 2 and 7 days post-caerulein injection (mean \pm SEM, $n = 5$). *Rplp0* and *Gapdh* were used as internal housekeeping gene controls. * $p < 0.05$ KRas versus WT mice; # $p < 0.05$ RKO versus KRas mice.

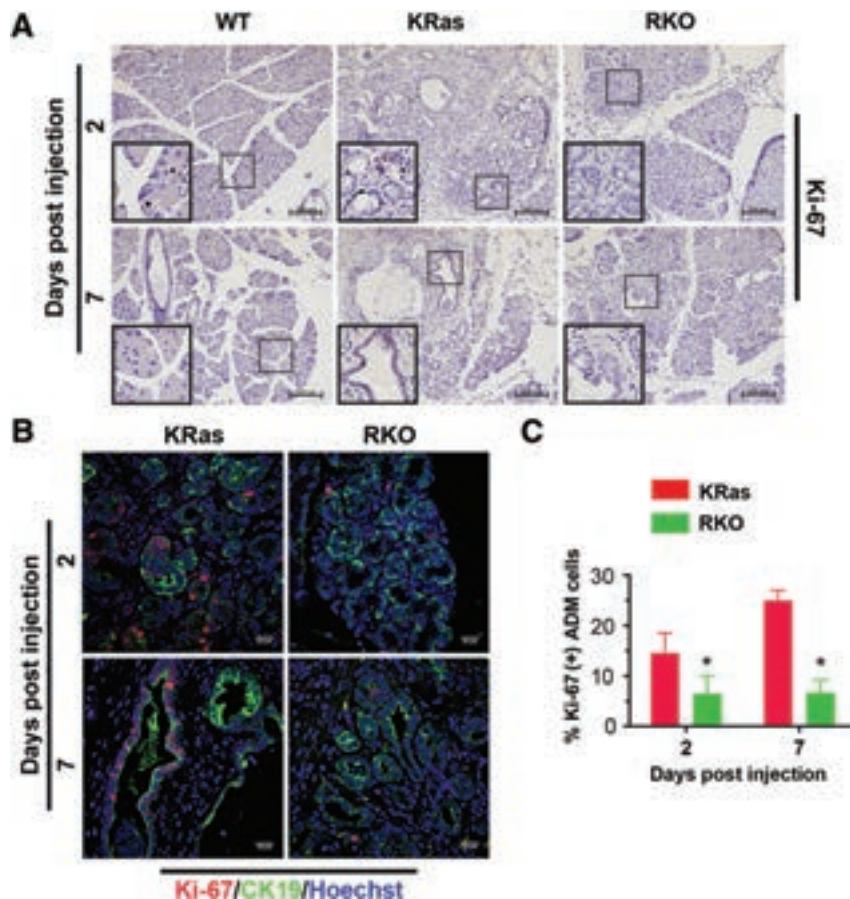


Figure 5. GSK-3 β contributes to the proliferation of ADM cells. (A) IHC staining for Ki-67 in WT, KRas, and RKO pancreas. Representative images were taken under 10 \times magnification lens. Bars = 200 μ m. (B) Double-labelling of pancreatic sections from KRas and RKO mice was performed 2 or 7 days post-caerulein injection using Ki-67 (red) and CK19 (green) antibodies. Nuclei were counterstained with Hoechst (blue). (C) Quantification of the percentage of Ki-67-positive ADM cells in KRas and RKO mice 2 or 7 days post-caerulein injection (mean \pm SEM, n = 6). * p < 0.05 RKO versus KRas mice.

contrast, RKO mice showed fewer Ki-67-positive cells in ADM and PanIN lesions (Figure 5A). The percentage of Ki-67-positive ADM cells, as determined by co-staining with CK19, is reduced in RKO mice compared with KRas mice at both day 2 and day 7 (Figure 5B, C). In addition, EdU labelling, which marks cells actively synthesizing DNA, showed a decrease in S-phase in RKO versus KRas mice at both day 2 and day 7 post-caerulein treatment (supplementary material, Figure S4C, D). We did not observe an increase in the number of apoptotic cells in ADM or PanIN lesions in RKO mice at either time point following caerulein injection (data not shown). Taken together, these data suggest that GSK-3 β is required for oncogenic *KRas*-driven cell proliferation within ADM and PanIN regions.

GSK-3 β facilitates proliferation through mTOR

Previous studies in breast cancer cell lines have shown that GSK-3 β cooperates with mammalian target of rapamycin (mTOR) to regulate the activity of ribosomal protein S6 kinase (S6 K), an important regulator of cell proliferation and growth [36]. We observed increased phosphorylation of the S6 K substrate S6 (pS6) from day 2 to day 7 post-caerulein treatment

in KRas mice compared with RKO mice (Figure 6A). Interestingly, more of the pS6-positive cells in the KRas mice are also CK19-positive compared with those in RKO mice (supplementary material, Figure S5A). In contrast, while pS6 and CK19 double-positive staining was observed in RKO mice at days 2 and 7, the majority of pS6-positive cells were negative for CK19 and resided outside the ADM area (Figure 6A and supplementary material, Figure S5A). These data indicate that deletion of GSK-3 β affects S6 K activity within the KRas-driven metaplastic duct cells.

To further examine the role of GSK-3 β in regulating S6 K activity, we treated AR42J pancreatic acinar tumour cells with the GSK3i in the presence and absence of caerulein stimulation. We found increased S6 phosphorylation on all four phosphorylation sites in the control group after caerulein stimulation for 2 or 6 h. Interestingly, we detected a decrease of S6 phosphorylation after GSK3i treatment (Figure 6B and supplementary material, Figure S5B). Similarly, knockdown of GSK-3 β in AR42J cells led to reduced phosphorylation of S6 after caerulein stimulation (Figure 6C and supplementary material, Figure S5C). Taken together, these data suggest that GSK-3 β regulates the activity of S6 K in response to caerulein stimulation.

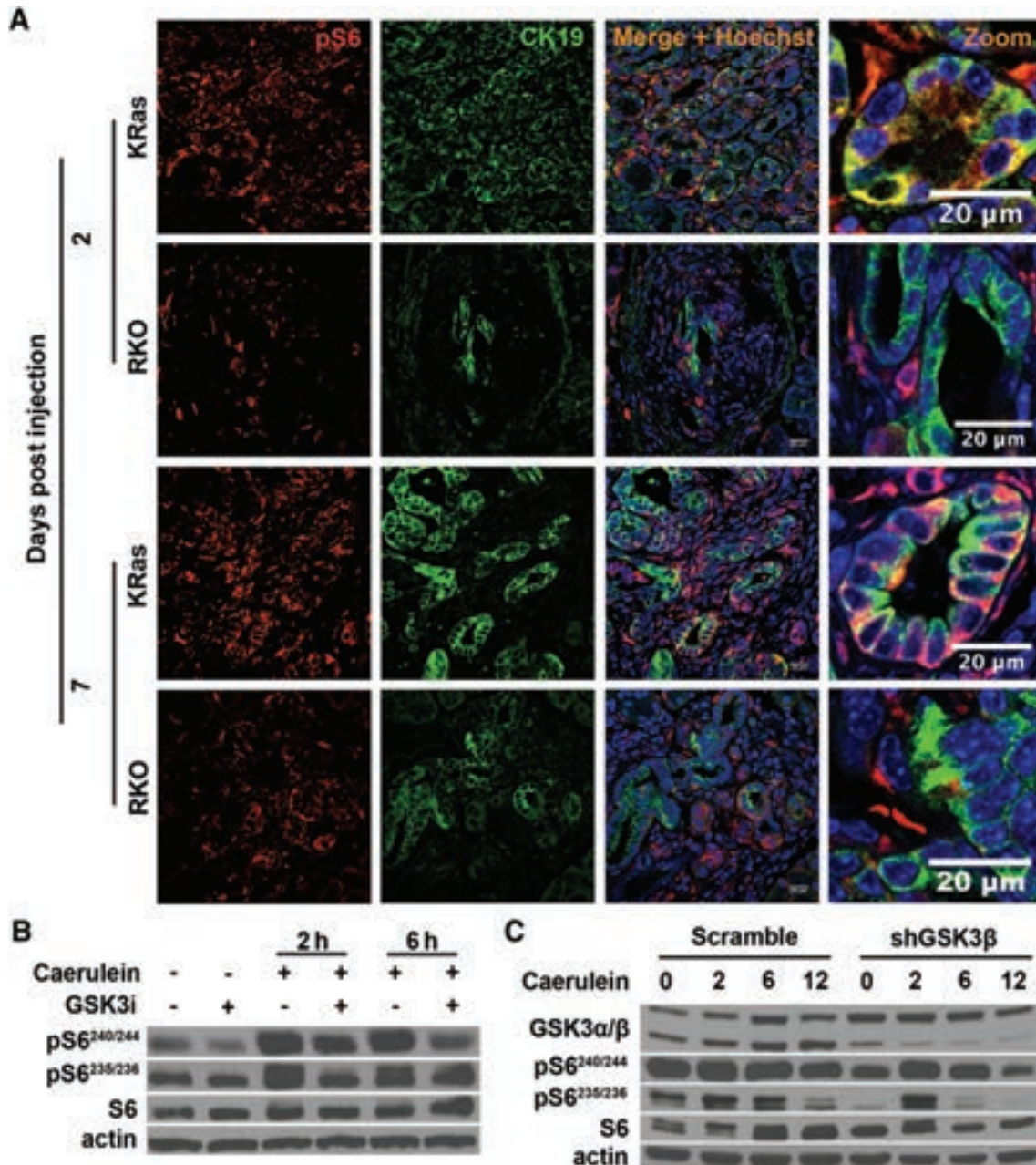


Figure 6. GSK-3 β deletion decreases the levels of phospho-S6. (A) Double-labelling of pancreatic sections derived from KRas and RKO mice 2 or 7 days post-caerulein injection for pS6 (red) and CK19 (green). Nuclei were counterstained with Hoechst (blue). (B) AR42J cells were pretreated with diluent (DMSO) or GSK-3i for 2 h and then with caerulein for an additional 2 or 6 h. Cell lysates were probed with the indicated antibodies. (C) Stable control and shGSK-3 β AR42J cells were treated with caerulein for 2, 6, and 12 h. Cell lysates were probed with the indicated antibodies. Representative results from six independent experiments are shown.

Discussion

The present study demonstrates a critical role for GSK-3 β in pancreatitis-induced ADM and PanIN lesion formation. This general conclusion is supported by the following distinct observations: (1) the expression of GSK-3 β is increased in caerulein-induced ADM areas and PanIN lesions; (2) acinar cells from GSK-3 β knockout mice form fewer ductal structures after TGF- α stimulation relative to WT acinar cells *in vitro*; (3) GSK-3 β ablation results in a reduction of caerulein-induced ADM development and PanIN

progression in *Kras*^{G12D} mice; (4) GSK-3 β deletion inhibits the proliferation of ADM cells driven by oncogenic *KRas*; and (5) GSK-3 β could in part stimulate proliferation of metaplastic ductal-like cells through activation of S6 K. These results highlight the role of GSK-3 β in the process of ADM and suggest that GSK-3 inhibitors may prove beneficial in abrogating these early events leading to the development of pancreatic cancer.

We have previously demonstrated that GSK-3 β becomes progressively overexpressed in PanIN lesions and PDAC patient samples. Consistent with a role for this kinase in PDAC, we and others have shown that

genetic or pharmacological inhibition of GSK-3 β abrogates the growth of PDAC cell lines *in vitro* and *in vivo* [20,22]. Significantly, we have previously reported that oncogenic *KRas*, which is present in more than 90% of PDACs, increases GSK-3 β gene expression [24]. Since oncogenic *KRas* has been shown to drive ADM both *in vivo* and *ex vivo*, we reasoned that GSK-3 β might be involved in altering the plasticity of pancreas cells during the process of ADM. Indeed, using the 3D explant *ex vivo* cell culture model, we showed that TGF- α -induced ADM is impaired by either pharmacological inhibition of GSK-3, specific knockdown of GSK-3 β , or when acinar cells from GSK-3 β conditional KO mice are used. Furthermore, we showed *in vivo* that GSK-3 β deletion reduces the extent of ADM and PanIN lesion progression in mice expressing oncogenic *KRas*. These results highlight an important role for GSK-3 β signalling downstream of oncogenic *KRas* during ADM and the formation of these preneoplastic lesions. As deletion of GSK-3 β did not completely abolish ADM and PanIN lesion formation in the presence of *KRas*, it remains possible that GSK-3 α might also be involved, but this will require further experimentation.

We have previously shown that co-injection of a GSK-3 inhibitor along with caerulein in oncogenic *KRas* mutant mice results in dose-dependent abrogation of pancreatitis and ADM formation [28]. GSK-3 β has multiple intracellular targets including several inflammatory transcription factors including NF κ B and NFAT (nuclear factor of activated T cells). Importantly, induced NFAT expression during ADM contributes to the development of PDAC by driving pathways involved in inflammation and proliferation and transcription factors involved in stemness including Sox2 and Sox9 [37–39], the latter factor being linked to PanIN lesion formation and the development of PDAC in the presence of oncogenic *KRas*. Whether GSK-3 β is involved in the regulation of SOX9 during the process of ADM remains to be determined. In addition, as the role of GSK-3 β in driving inflammation is well known, it remains possible that decreased expression of inflammatory signature genes in the absence of GSK-3 β could impact sustained ADM development and the extent of inflammation in our model. In fact, previous studies have shown that GSK-3 inhibitors diminished inflammatory responses in experimentally induced colitis in rats [40], as well as arthritis and peritonitis in mice [41]. Future experiments aimed at identifying the transcriptional networks regulated by GSK-3 β during ADM development will provide valuable insight into the role of this kinase in supporting pancreatitis and the development of PDAC.

Another feature of GSK-3 β loss in our model is the decrease in proliferation of duct-like cells within the ADM areas and PanIN lesions. Interestingly, while many Ki-67⁺ cells in the *KRas* mice are also CK19⁺, this is not the case in RKO mice, suggesting a critical role of GSK-3 β in driving the proliferation of the metaplastic duct-like cells in the presence of oncogenic *KRas*. Mechanistically, we have provided evidence that GSK-3 β affects the activity of S6 K. S6 K is known

to stimulate mRNA translation, protein synthesis, and proliferation, but GSK-3 β regulation of S6 K is controversial. Inoki *et al.* showed that GSK-3 β negatively regulated phosphorylation of S6 K at T389 by activating TSC, an upstream negative regulator of mTOR [42]. However, Shin *et al.* established that GSK-3 β directly phosphorylates S6 K1 at S371, resulting in increased phosphorylation of its downstream substrate, S6 [36]. Consistent with this, we found increased phosphorylation of S6 in CK19⁺ cells within the ADM and PanIN lesions of *KRas* mice, which was lost in the RKO mice. Moreover, while pS6⁺ cells were observed in the RKO mice, most cells containing the highest levels of pS6 were not CK19⁺, suggesting that GSK-3 β is important for maintaining S6 K activity in metaplastic duct-like cells.

In summary, our study provides evidence that GSK-3 β is necessary to mediate TGF- α - and *KRas* mutation-induced pancreatic cellular plasticity leading to ADM and the formation of PanIN lesions. In addition, GSK-3 β contributes to the proliferation of these metaplastic duct-like cells in part through the regulation of S6 K activity. Thus, targeting GSK-3 β pharmacologically might have clinical benefit in removing or eliminating these precursor cells during different diseased states.

Acknowledgements

This work was supported by grants from NCI Pancreatic Cancer SPORE (grant CA102701, to DDB), the National Natural Science Foundation of China (grant No 81472601, to JSZ), and NCI (grant No CA200572, to PS). The rat pancreatic acinar tumour AR42J cells were a gift from Dr Raul Urrutia (Mayo Clinic). *Pdx1-Cre;LSL-KRas^{G12D}* mice were obtained from Dr Baoan Ji (Mayo Clinic) and GSK-3 $\beta^{F/F}$ mice were obtained from Dr James Woodgett (Mount Sinai Hospital, Toronto, Canada).

Author contributions statement

The authors contributed in the following way: LD: study concept and design, data acquisition, analysis and interpretation, drafting the manuscript, and critical revision of the manuscript for important intellectual content; GYL and PS: contribution to data acquisition, analysis and interpretation, and technical and material support; J-SZ: study concept and design, data acquisition, analysis and interpretation, technical support, study supervision, drafting the manuscript, and critical revision of the manuscript; DMS: provision of key reagents, technical and material support, and editing of the manuscript; DDB: study concept and design, data acquisition, analysis and interpretation, drafting the manuscript, critical revision of the manuscript for important intellectual content, obtainment of funding, technical support, study supervision, and guarantor of this work.

References

- Rahib L, Smith BD, Aizenberg R, et al. Projecting cancer incidence and deaths to 2030: the unexpected burden of thyroid, liver, and pancreas cancers in the United States. *Cancer Res* 2014; **74**: 2913–2921.
- Ryan DP, Hong TS, Bardeesy N. Pancreatic adenocarcinoma. *N Engl J Med* 2014; **371**: 2140–2141.
- Wolfgang CL, Herman JM, Laheru DA, et al. Recent progress in pancreatic cancer. *CA Cancer J Clin* 2013; **63**: 318–348.
- Morris JPt, Wang SC, Hebrok M. KRAS, Hedgehog, Wnt and the twisted developmental biology of pancreatic ductal adenocarcinoma. *Nat Rev Cancer* 2010; **10**: 683–695.
- Kanda M, Matthaehi H, Wu J, et al. Presence of somatic mutations in most early-stage pancreatic intraepithelial neoplasia. *Gastroenterology* 2012; **142**: 730–733.e739.
- Guerra C, Schuhmacher AJ, Canamero M, et al. Chronic pancreatitis is essential for induction of pancreatic ductal adenocarcinoma by K-Ras oncogenes in adult mice. *Cancer Cell* 2007; **11**: 291–302.
- Reichert M, Rustgi AK. Pancreatic ductal cells in development, regeneration, and neoplasia. *J Clin Invest* 2011; **121**: 4572–4578.
- Hingorani SR, Petricoin EF, Maitra A, et al. Preinvasive and invasive ductal pancreatic cancer and its early detection in the mouse. *Cancer Cell* 2003; **4**: 437–450.
- Wagner M, Luhrs H, Kloppel G, et al. Malignant transformation of duct-like cells originating from acini in transforming growth factor transgenic mice. *Gastroenterology* 1998; **115**: 1254–1262.
- Carriere C, Seeley ES, Goetze T, et al. The Nestin progenitor lineage is the compartment of origin for pancreatic intraepithelial neoplasia. *Proc Natl Acad Sci U S A* 2007; **104**: 4437–4442.
- Zhu L, Shi G, Schmidt CM, et al. Acinar cells contribute to the molecular heterogeneity of pancreatic intraepithelial neoplasia. *Am J Pathol* 2007; **171**: 263–273.
- Gidekel Friedlander SY, Chu GC, Snyder EL, et al. Context-dependent transformation of adult pancreatic cells by oncogenic K-Ras. *Cancer Cell* 2009; **16**: 379–389.
- Strobel O, Dor Y, Alsina J, et al. *In vivo* lineage tracing defines the role of acinar-to-ductal transdifferentiation in inflammatory ductal metaplasia. *Gastroenterology* 2007; **133**: 1999–2009.
- Cano DA, Hebrok M, Zenker M. Pancreatic development and disease. *Gastroenterology* 2007; **132**: 745–762.
- Collins MA, Bednar F, Zhang Y, et al. Oncogenic Kras is required for both the initiation and maintenance of pancreatic cancer in mice. *J Clin Invest* 2012; **122**: 639–653.
- Jope RS, Yuskaitis CJ, Beurel E. Glycogen synthase kinase-3 (GSK3): inflammation, diseases, and therapeutics. *Neurochem Res* 2007; **32**: 577–595.
- Doble BW, Woodgett JR. GSK-3: tricks of the trade for a multi-tasking kinase. *J Cell Sci* 2003; **116**: 1175–1186.
- McCubrey JA, Steelman LS, Bertrand FE, et al. GSK-3 as potential target for therapeutic intervention in cancer. *Oncotarget* 2014; **5**: 2881–2911.
- Takahashi-Yanaga F. Activator or inhibitor? GSK-3 as a new drug target. *Biochem Pharmacol* 2013; **86**: 191–199.
- Ougolkov AV, Fernandez-Zapico ME, Bilim VN, et al. Aberrant nuclear accumulation of glycogen synthase kinase-3 β in human pancreatic cancer: association with kinase activity and tumor dedifferentiation. *Clin Cancer Res* 2006; **12**: 5074–5081.
- Ougolkov AV, Fernandez-Zapico ME, Savoy DN, et al. Glycogen synthase kinase-3 β participates in nuclear factor κ B-mediated gene transcription and cell survival in pancreatic cancer cells. *Cancer Res* 2005; **65**: 2076–2081.
- Garcea G, Manson MM, Neal CP, et al. Glycogen synthase kinase-3 beta; a new target in pancreatic cancer? *Curr Cancer Drug Targets* 2007; **7**: 209–215.
- Mishra R. Glycogen synthase kinase 3 beta: can it be a target for oral cancer. *Mol Cancer* 2010; **9**: 144.
- Zhang JS, Koenig A, Harrison A, et al. Mutant K-Ras increases GSK-3 β gene expression via an ETS-p300 transcriptional complex in pancreatic cancer. *Oncogene* 2011; **30**: 3705–3715.
- Hoefflich KP, Luo J, Rubie EA, et al. Requirement for glycogen synthase kinase-3 β in cell survival and NF- κ B activation. *Nature* 2000; **406**: 86–90.
- MacAulay K, Doble BW, Patel S, et al. Glycogen synthase kinase 3 α -specific regulation of murine hepatic glycogen metabolism. *Cell Metab* 2007; **6**: 329–337.
- Zhang JS, Herreros-Villanueva M, Koenig A, et al. Differential activity of GSK-3 isoforms regulates NF- κ B and TRAIL- or TNF α induced apoptosis in pancreatic cancer cells. *Cell Death Dis* 2014; **5**: e1142.
- Baumgart S, Chen NM, Zhang JS, et al. GSK-3 β governs inflammation-induced NFATc2 signaling hubs to promote pancreatic cancer progression. *Mol Cancer Ther* 2016; **15**: 491–502.
- Liou GY, Doppler H, Necela B, et al. Macrophage-secreted cytokines drive pancreatic acinar-to-ductal metaplasia through NF- κ B and MMPs. *J Cell Biol* 2013; **202**: 563–577.
- Means AL, Meszoely IM, Suzuki K, et al. Pancreatic epithelial plasticity mediated by acinar cell transdifferentiation and generation of nestin-positive intermediates. *Development* 2005; **132**: 3767–3776.
- Ding L, Yin Y, Han L, et al. TSC1–mTOR signaling determines the differentiation of islet cells. *J Endocrinol* 2017; **232**: 59–70.
- Doble BW, Patel S, Wood GA, et al. Functional redundancy of GSK-3 α and GSK-3 β in Wnt/ β -catenin signaling shown by using an allelic series of embryonic stem cell lines. *Dev Cell* 2007; **12**: 957–971.
- Carriere C, Young AL, Gunn JR, et al. Acute pancreatitis markedly accelerates pancreatic cancer progression in mice expressing oncogenic Kras. *Biochem Biophys Res Commun* 2009; **382**: 561–565.
- Shi C, Washington MK, Chaturvedi R, et al. Fibrogenesis in pancreatic cancer is a dynamic process regulated by macrophage–stellate cell interaction. *Lab Invest* 2014; **94**: 409–421.
- Kuroki H, Hayashi H, Okabe H, et al. EZH2 is associated with malignant behavior in pancreatic IPMN via p27^{Kip1} downregulation. *PLoS One* 2014; **9**: e100904.
- Shin S, Wolgamott L, Yu Y, et al. Glycogen synthase kinase (GSK)-3 promotes p70 ribosomal protein S6 kinase (p70S6 K) activity and cell proliferation. *Proc Natl Acad Sci U S A* 2011; **108**: E1204–E1213.
- Hessmann E, Zhang JS, Chen NM, et al. NFATc4 regulates Sox9 gene expression in acinar cell plasticity and pancreatic cancer initiation. *Stem Cells Int* 2016; **2016**: 5272498.
- Singh SK, Chen NM, Hessmann E, et al. Antithetical NFATc1–Sox2 and p53–miR200 signaling networks govern pancreatic cancer cell plasticity. *EMBO J* 2015; **34**: 517–530.
- Chen NM, Singh G, Koenig A, et al. NFATc1 links EGFR signaling to induction of Sox9 transcription and acinar–ductal transdifferentiation in the pancreas. *Gastroenterology* 2015; **148**: 1024–1034.e1029.
- Hofmann C, Dunger N, Scholmerich J, et al. Glycogen synthase kinase 3- β : a master regulator of toll-like receptor-mediated chronic intestinal inflammation. *Inflamm Bowel Dis* 2010; **16**: 1850–1858.
- Hu X, Paik PK, Chen J, et al. IFN- γ suppresses IL-10 production and synergizes with TLR2 by regulating GSK3 and CREB/AP-1 proteins. *Immunity* 2006; **24**: 563–574.
- Inoki K, Ouyang H, Zhu T, et al. TSC2 integrates Wnt and energy signals via a coordinated phosphorylation by AMPK and GSK3 to regulate cell growth. *Cell* 2006; **126**: 955–968.

SUPPLEMENTARY MATERIAL ONLINE**Supplementary figure legends**

Figure S1. GSK3i treatment impairs acinar-to-duct formation in response to TGF- α

Figure S2. GSK-3 β deletion does not alter the subcellular localization of β -catenin or result in increased expression of β -catenin target genes

Figure S3. GSK-3 β deletion impairs ADM and PanIN lesion formation in response to acute inflammation

Figure S4. GSK-3 β deletion decreases cell proliferation

Figure S5. GSK-3 β deletion reduces the levels of pS6 in caerulein-treated mice and AR42J cells

Table S1. Antibody details

Table S2. Primers used for real-time PCR analysis